Mon. Not. R. astr. Soc. (1986) **221,** 993–1000

Molecular hydrogen mapping of Herbig–Haro 7–11; a filamentary bullet?

J. F. Lightfoot and W. M. Glencross *Department of Physics and Astronomy, University College London, Gower Street, London WC1E 6BT*

Accepted 1986 April 12. Received 1986 April 2; in original form 1985 November 28

Summary. A map is presented of the Q-branch H_2 line emission associated with Herbig–Haro 7–11. The molecules are shock-excited and the emitting area stretches 4 arcmin north-west from HH7–11 in a fairly sharp and straight line. The evidence suggests that the emission occurs where a spine of dense molecular gas is being struck by a jet from the young star SVS13.

The origin of the Herbig–Haro objects is discussed. We suggest that HH7–11 are the bow-shocks formed around a helical filament of dense gas moving at 200 km s^{-1} through the molecular cloud. The filament could be produced by a well-collimated precessing jet from SVS13. HH2, HH12 and HH101 may be explained in a similar way.

1 Introduction

It has become clear in the past few years that any young stars pass through phases of energetic mass outflow (Bally & Lada 1983); Herbig–Haro (HH) objects and high-velocity molecular line emission are two observable consequences. Despite the large number of observations made, the energetics and gas dynamics of the flows are still poorly understood. In particular, the relationship between the very high velocity gas responsible for the HH objects and the lower velocity molecular flows is far from clear. With this in mind, we have examined the area around HH7–11 in the near-infrared emission lines of shocked H_2. The small beamwidths available and the low obscuration at these wavelengths make such mapping an attractive way of showing up the overall shock structure in outflow sources.

2 Observations and results

The observations were made using a Circular Variable Filter at UKIRT on 1984 September 12–13. The spectral resolution of the instrument was 0.85 per cent, and the circular field of view was 19.6 arcsec in diameter. An east–west spatial chop was used with an amplitude of 190 arcsec.

The map was made in a blend of the $v=1$–0 Q-branch lines near 2.43 μm. The line flux at each point was measured relative to the continuum at 2.39 μm, which was nearly always negligible, and

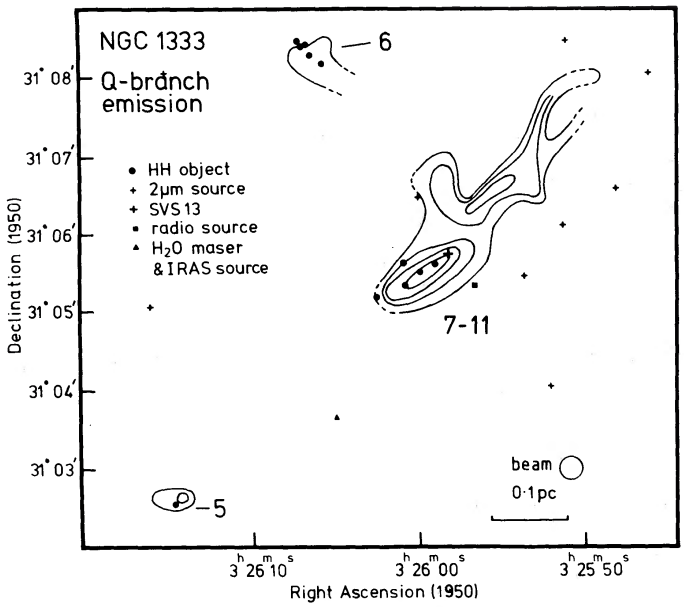

Figure 1. A map of the Q-branch H_2 emission from the area around Herbig–Haro 7–11. Contours are at 2, 4, 8 and 16σ; 1σ is 10^{-21} W cm^{-2}, measured in a 0.007 μm band centred at 2.43 μm.

calibrated using measurements of HD 225023 (Elias *et al.* 1982). Sampling was on a regular grid pattern with 20 arcsec spacing and the integration time on the line was 40 s at each map point. The map is shown in Fig. 1, while Plate 1 shows the H_2 contours superimposed on a photograph of the region. The fully surveyed area does not extend far beyond the lowest contour plotted, although the nearby H_2O masers, some *IRAS* sources, and a few points between HH7–11 and HH5 were also examined.

In addition, spectra between 2.0 and 2.5 μm were taken of the emission from HH5, HH7–11 and a point on the intensity peak north-west of HH7–11; these are given in Fig. 2(a), (b) and (c). The integration time per spectral point was 12 s and the data were again calibrated using HD 225023.

3 Overall structure

HH7–11 is a group of objects associated with a young star in the dark cloud Lynds 1450. Another part of this cloud is illuminated by a nearby B star to produce the reflection nebula NGC 1333. A distance to the cloud of 350 pc has been adopted by Herbig & Jones (1983).

Photometric surveys at 2 μm have revealed a number of stars embedded in the cloud (Strom, Vrba & Strom 1976; Cohen & Schwartz 1980). One of these, SVS13, lying at the end of the chain of HH objects, is associated with H_2O maser emission (Haschick *et al.* 1983) and is almost certainly the young star driving the HH7–11 outflow (see Fig. 1). Another object in the vicinity, which shows up in radio continuum and H_2O maser observations (Haschick *et al.* 1980), could also be a source of high-velocity gas. The radio emission clearly does not derive from a conventional H II region surrounding a B star ($L \sim 2000\,L_\odot$) since *IRAS* observations give this object and SVS13 a combined luminosity of only 58 $L_\odot$ (Jennings *et al.* 1986). The radio flux must, therefore, originate either in the ionized wind from a heavily obscured star (Cohen, Bieging & Schwartz 1982) or in a buried, high-excitation HH object (Pravdo *et al.* 1985).

Optical observations (Mundt 1986) show that HH11, 10, 8 and 7 lie along a curve. Only HH9, which is faint compared to the rest, lies off the track. All the objects lie in a cone of faint diffuse emission which grows stronger towards HH7. This appearance is consistent with the presence of a

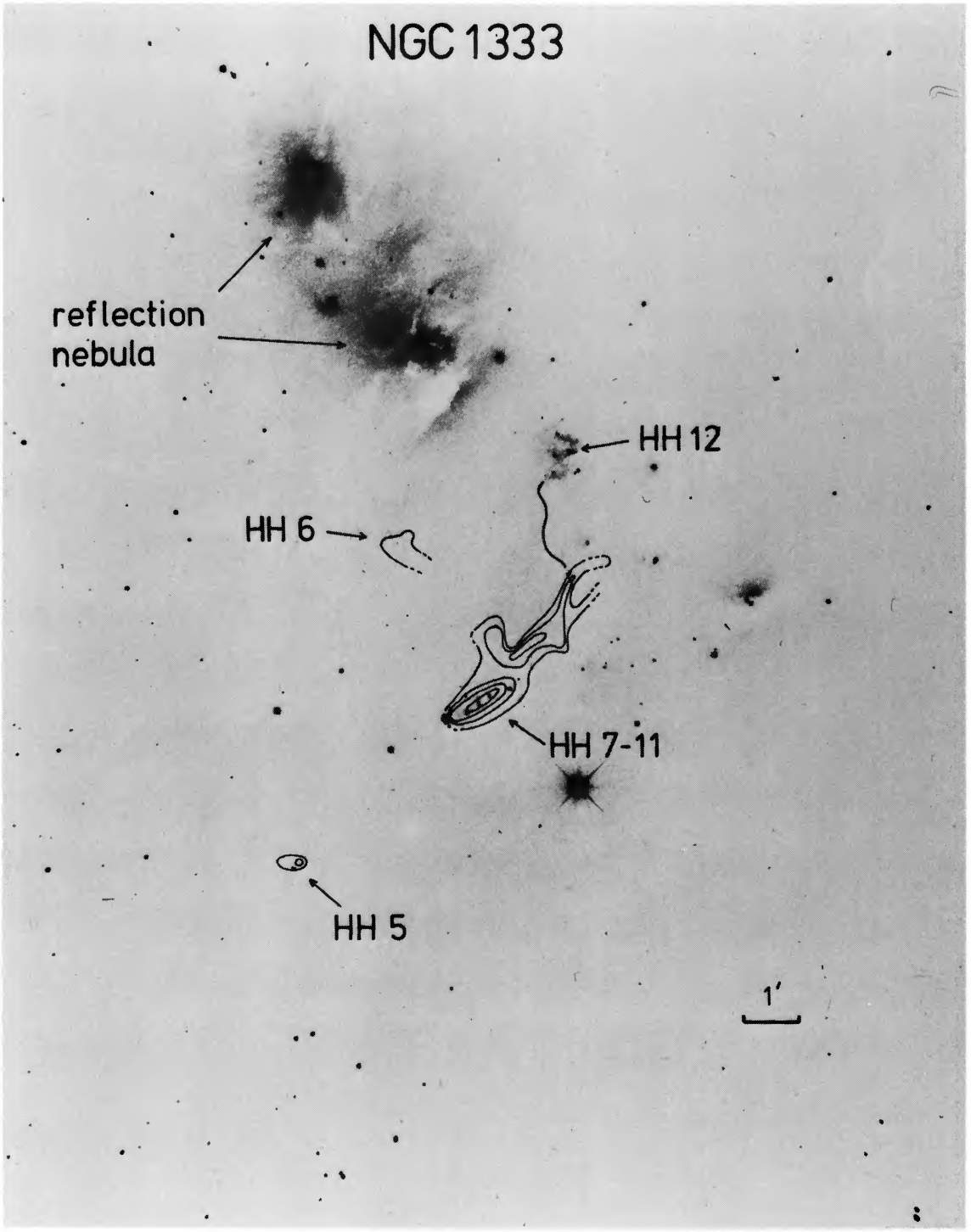

Plate 1. The contours of H_2 Q-branch emission are shown superimposed on a photograph of the region provided by G. H. Herbig. The path of the Hα filament is also indicated.

[*facing page* 994]

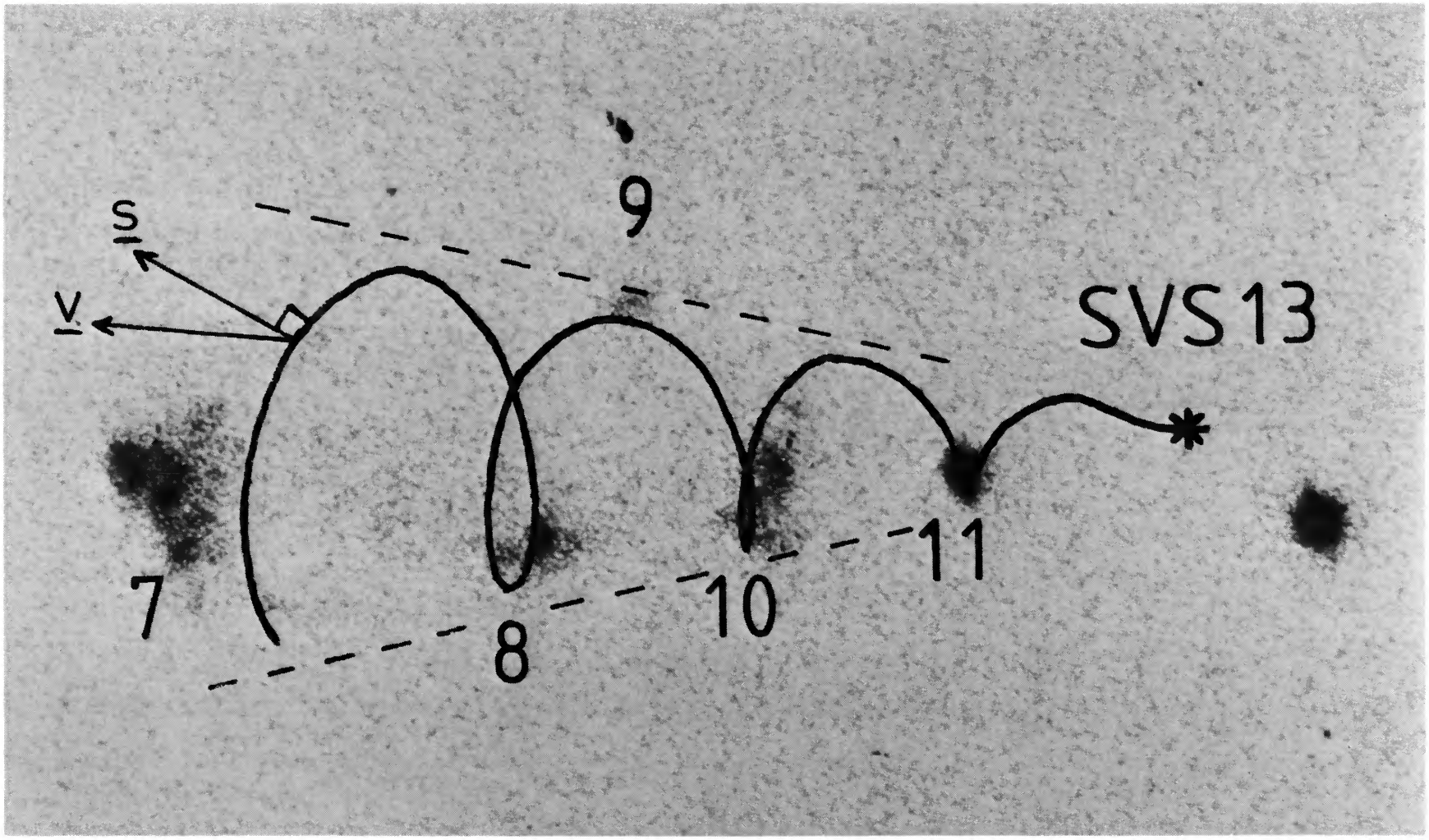

Plate 2. The thick line illustates the shape of a regular helical jet expanding away from SVS13. The helix has an opening angle of 12° and its axis is tilted towards the observer by 30° out of the plane of the sky. It is superimposed on a photograph of HH7–11 supplied by G. H. Herbig. Dashed lines indicate the extent of the diffuse optical cone mentioned in the text. The vector **v** represents the velocity of the gas forming the helix (which is moving directly away from SVS13), while **s** is the effective velocity of the resultant bow-shock.

roughly conical volume of disturbance leading away from SVS13 (perhaps a cavity similar to that apparent in L1551; Strom *et al.* 1985).

HH11 has a proper motion corresponding to a cross-sky velocity of 58 km s^{-1} away from SVS13 (Herbig & Jones 1983); reliable measurements of the proper motions of the other objects have not been possible because of their greater size and complexity. Strom, Grasdalen & Strom (1974) found the radial velocity of the gas in the objects to vary between -146 km s^{-1} in HH11 and -29 km s^{-1} in HH10, with no obvious trend apparent.

HH7 and 11 show emission spectra characteristic of a low-velocity (~ 40 km s^{-1}) plane shock wave moving into pre-shock gas with $n_H = 10^3$–10^4 cm^{-3} (Bohm, Brugel & Olmsted 1983; Dopita, Binette & Schwartz 1982). Using the optical data of Bohm *et al.* (1983) and assuming that ~ 90 per cent of the shock cooling occurs in UV line and continuum emission yields a luminosity for each object of 0.05 $L_\odot$. HH7 is a low-excitation object, which suggests that it is not the working surface of the stellar flow.

The observed ratio of the H_2 $v=2$–1 and $v=1$–0 $S(1)$ lines (~ 0.1) from the region is consistent with H_2 excitation by shock heating rather than by UV fluorescent pumping (Black & Dalgarno 1976). As can be seen from Fig. 1, the main limb of H_2 emission is long, thin and remarkably straight overall, apart from the faint spur north of HH7–11. On a smaller scale some distortion is apparent. In particular, the long axis of the H_2 emission is not well aligned with the diffuse optical cone around HH7–11, though the detailed correspondence between the HH objects and the H_2 intensity is very good.

Heavy obscuration probably explains the lack of optical emission from the north-western H_2 limb. An estimate of the absorption in this region may be obtained by assuming that the H_2 excitation temperature is constant across the nebula, and that the extinction varies as $\lambda^{-1.7}$ (van de Hulst extinction curve No. 15), in which case the observed ratios of the $v=1$–0 $S(1)$ and Q-branch lines indicate an A_V of 10 ± 5 mag relative to HH7–11.

The H_2 emission around HH7–11 has an integrated $S(1)$ luminosity of 0.01 $L_\odot$ which, if the H_2 level populations are in LTE at 2000 K, implies a luminosity in all H_2 lines of $\sim 0.1\,L_\odot$. The corresponding luminosities for the north-western lobe and HH5 are 0.2 and $6 \times 10^{-3}\,L_\odot$. The area of the H_2 emitting region is not determined by our observations, but reasonable lower and upper limits are given by the combined area of the HH objects (~ 60 arcsec^2) and the area of the diffuse optical cone (~ 500 arcsec^2). The corresponding $S(1)$ line surface brightness lies between 1.9×10^{-3} and 3×10^{-4} erg cm^{-2} s^{-1} sr^{-1} which, from the models of Draine, Roberge & Dalgarno (1983), implies a 30–40 km s^{-1} shock wave moving into gas with $n_H = 10^4$ cm^{-3}. These velocities are close to the dissociation limit for H_2 shocks. The similarity between the optical and H_2 shock parameters suggests that one shock may be responsible for both types of emission.

Bipolar high-velocity CO emission was detected and mapped over a large area with a 1 arcmin beam by Snell & Edwards (1981) and Edwards & Snell (1983). A blueshifted lobe includes HH7–11, while the major part of the redshifted gas covers the long north-western H_2 limb. Similar CO mapping with a 30 arcsec beam has since been performed by Liseau & Sandell (1986) over the small area around HH7–11 and SVS13. This work has revealed that the CO flow does not follow a straight line through SVS13 and that the blueshifted CO covers a larger area than the optical and H_2 emission. Furthermore, there is a limb of redshifting CO extending into the HH7–11 blue lobe and an area of blueshifted gas in the red lobe 1 arcmin north-west of SVS13. The overall impression is that the movement of molecular gas is not symmetric around SVS13, nor is all the gas moving radially from the star.

Maps of NH_3 and $C^{18}O$ emission (Schwartz, Bologna & Smith 1983; Schwartz, Waak & Smith 1983) show a molecular ridge extending about 8 arcmin to the south-east of SVS13. The feature is narrow and very well aligned with the long H_2 limb. The line profiles show the emitting gas to be static, in which case the ridge probably marks an extension to the NGC 1333 molecular cloud

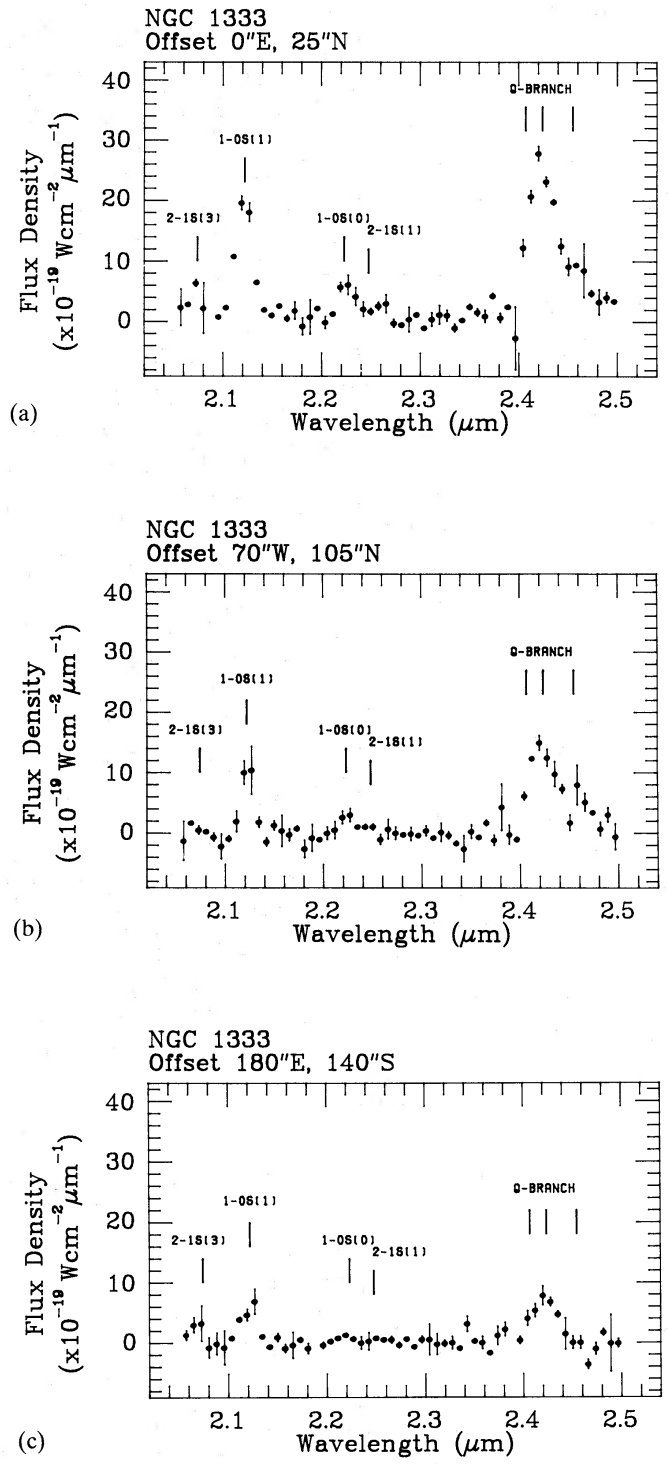

Figure 2. (a) The *K*-window spectrum of the H_2 emission from a point near SVS13. The position offset is from $\alpha(1950) = 3^h 26^m 00^s$, $\delta(1950) = +31° 05' 00''$. (b) The spectrum at the peak of the north-western H_2 emission limb. (c) The spectrum of the H_2 emission around HH5.

rather than a dense shell swept up by the SVS13 outflow. Since the H_2 column density in the ridge is approximately 3×10^{21} cm^{-2} (Schwartz *et al.* 1983) and gas densities in excess of 5×10^3 cm^{-3} are required to excite the NH_3 emission, the implied line-of-sight depth through the feature is 6×10^{17} cm or less. This is similar to the apparent width of the ridge, indicating that it is a spine of

molecular gas rather than a flat plate seen edge-on. The spine may well extend further to the north-west of SVS13 than is apparent from the observations, which are confused by emission from the main body of the NGC 1333 cloud in this area. CS observations by Schwartz *et al.* (1983) show that SVS13 itself has formed in a dense clump ($n_H \geqslant 10^5\,cm^{-3}$), presumably within the spine. The entire NGC 1333 cloud complex is suffused by a halo of low-density gas ($n_H \sim 500\,cm^{-3}$).

A deep CCD image of the region in Hα shows an emission filament snaking away from the end of the north-western H_2 limb up to HH12 (Strom, Strom & Stocke 1983). Further observations by these authors reveal high blueshifted gas velocities in the filament ($\sim 100\,km\,s^{-1}$) and suggest a turn-over in the radial velocity (from blue to redshifted) around a certain M star. This is taken to imply that this star is the source of the high-velocity gas, in which case the northern part of the H_2 limb might mark the impact of the opposite jet on the SVS13 molecular cloud. However, the low luminosity of the M star ($\sim 0.3\,L_\odot$) compared to that of SVS13 ($\sim 58\,L_\odot$) is difficult to reconcile with the similar optical brightnesses of HH12 and HH7–11. In addition, since it is possible (see Section 4) that the stellar flow responsible for HH7–11 takes the form of a jet from SVS13 whose direction has shifted considerably with time, it is not impossible that the opposite jet from SVS13 is responsible both for the blueshifted Hα filament and the H_2 emission in the redshifted CO lobe. We can only conclude that the relationship between HH12 and SVS13 will remain unclear until further velocity information has been obtained on the Hα filament and the north-western H_2 limb.

There is similar uncertainty regarding the possible association of HH5 with the HH7–11 system. This object is situated in line with HH7–11 and its proper motion lies directly away from SVS13 (Jones 1983). However, another young star, seen as an *IRAS* peak and H_2O maser, also lies nearby and cannot be ruled out as HH5's power source.

A final point regarding the source structure is that the H_2 emission may not delineate the whole of the stellar flow from SVS13. The H_2 flux around HH7–11 is closely correlated with the optical objects, but these lie along the edge of the diffuse optical cone leading from SVS13. Since the lifetime of the excited H_2 is short (~ 1 yr), this indicates that direct contact between the stellar wind and dense cloud is occurring today only along one edge of the cone of disturbed gas. Presumably the stellar flow has swept through the entire cone in the past and, perhaps, continues to do so but produces no emission because the dense ambient gas has been dissipated. It is likely that a similar situation prevails in the red lobe and that this H_2 also marks only part of the volume swept by the stellar flow. In this case the large-scale alignment of the red lobe H_2 limb may reflect the presence of dense molecular material only along this direction. This is consistent with the formation of SVS13 in a spine of molecular gas as suggested earlier. Similarly, the cut-off in the blueshifted optical, H_2 and high-velocity CO emission at HH7 could be explained by a drop in the density of the ambient gas beyond this point.

4 What are HH7–11?

Although a wide range of alternative explanations have been put forward for HH objects (see Schwartz 1978; Norman & Silk 1979), the following discussion is restricted to models involving protostellar jets. This is because there is firm evidence that jets are emitted by many young stars (e.g. Mundt 1986), and because it is found that such models are the only ones which can explain the regular spacing and shapes of HH7–11 without invoking an unsteady flow from the central star or an improbable distribution of circumstellar material. The evidence that SVS13 is producing a jet would be overwhelming if HH12 could be shown to be part of the same system, since it is difficult to put forward any other explanation for its associated Hα filament.

As a basis for further discussion, we assume that the jet is well collimated, neutral, has a velocity of $200\,km\,s^{-1}$, a number density of $10^6\,cm^{-3}$, and a temperature of 10^3 K. These figures are rather uncertain but are consistent with observations of this and similar sources (e.g. Bieging

& Cohen 1985). With these parameters, the jet has an internal sound speed of 2 km s^{-1} and a Mach number, M, of 100. The discussion which follows requires the blueshifted jet to have a mechanical luminosity of about 5 $L_\odot$, which implies a jet radius of 10^{15} cm (0.2 arcsec at 350 pc) and a total mass-loss rate from SVS13 of $\sim 3\times10^{-6} M_\odot$ yr^{-1}.

The basic behaviour of a supersonic jet is well known. Left to itself the jet expands or contacts at an opening angle differing from its initial value by, at most, $2/M$. Since this additional angle is only $\sim 1°$ for a Mach 100 jet, a highly collimated jet will remain narrow over a considerable distance if it is not disrupted by its interaction with the interstellar medium. This is consistent with the appearance of many protostellar jets (Mundt 1986).

We examine first the possibility that the HH objects are the static shock cells characteristic of under-expanded supersonic jets (e.g. Sanders 1983; Falle & Wilson 1985). The shock structure recurs at a spatial wavelength of roughly $M \times r$ (where r is the mean jet radius), which corresponds to about 20 arcsec for a jet of the above dimensions. This is close to the observed separations between HH7–11. However, in this case the shock surfaces would be a set of long thin cones along the jet axis, which is not consistent with the lateral spread of HH7 and 10. Nor is the singular radial velocity of HH11 readily explained.

The development of Kelvin–Helmholtz instabilities at the boundary between the jet and ambient cloud (Ferrari, Trussoni & Zaninetti 1983, and references therein) is also a potentially attractive explanation for HH7–11. Linear analysis shows that the fastest growing modes of instability in our narrow model jet occur at spatial wavelengths of about 10–20 arcsec, again close to the spacing of HH7–11. Any kink which develops at the flow boundary will drive oblique shocks into the jet and ambient cloud, which could produce the observed optical, H_2 and high-velocity CO emission. However this model also fails to explain the lateral extension of some of the HH objects and the rogue velocity of HH11.

Finally, we consider the possibility that the HH7–11 group is a member of the helical family of HH objects, exemplified by HH12 and HH101 (Morgan *et al.* 1984). We suggest that the sinuous optical structure of these sources can be explained as the bow shock around a dense helical filament, produced by a precessing jet source, advancing through the interstellar medium. Shocked H_2 and high-velocity CO emission will also result from this interaction. In the case of the HH7–11 group, we suggest further that a large conical cavity has been excavated from the cloud during the previous meanderings of the jet, so that today there is only a strong interaction where the outflow meets the wall of the cone or some wandering blob of material. Thus, the regularly spaced objects HH7, 8, 10 and 11 would lie along the line where the helix has hit the wall of the cone, while HH9 marks the position of an isolated molecular knot. Plate 2 illustrates the helix which might be producing HH7–11.

We assume that the effective velocity of the bow-shock at each point along the helix is the component of the filament velocity (assumed to be directly away from SVS13) orthogonal to the filament at that point (see Plate 2). Thus, at the position suggested for HH11, where the filament is at an angle of 30° to the direction of motion, the bow-shock peak velocity is only 100 km s^{-1} for a 200 km s^{-1} jet. For a regular helix the shock speed increases rapidly with distance from the powering star, so that the bow-shock velocity would be 190 km s^{-1} at HH7. These velocities are much higher than the 40 km s^{-1} deduced from the optical spectra of HH7 and 11, but it is known that the application of plane shock models to bow-shocks does lead to a severe underestimate of the bow-shock velocity (Hartmann & Raymond 1984).

The H_2 emission according to this model arises in the more oblique sections of the bow-shock, downsteam of those responsible for the optical lines. In this case further investigation of the H_2 spectrum should reveal characteristics of a range of shock-wave velocities. The proximity of UV emission from other parts of the bow-shock may also disturb the H_2 spectra (Jordan *et al.* 1978; Shull 1978).

Since the shocks in this model are in the ambient gas, the derived shock parameters provide no information on the jet itself. All that is required is that it be energetic enough to sustain the luminosity of the shocks over the observed length-scale of the phenomenon. The $5\,L_\odot$ mechanical luminosity assumed earlier for the blue jet from SVS13 would be adequate for this purpose.

To sum up, we feel that the helical jet model is the most attractive explanation for HH7–11 in the light of present knowledge. To confirm or disprove this, or any other, interpretation will require further data on the excitation and velocity structure of all the HH objects.

The possible application of this model to HH101 and HH12 has been mentioned already. Perhaps the best example of the type, however, is HH2. The series of bright knots which form this object do appear to lie along a helix and, furthermore, the emission spectrum and velocity structure of the individual knots are consistent with excitation in a 200–350 km s^{-1} bow-shock (Hartmann & Raymond 1984; Choe, Bohm & Solf 1985; Bohm & Solf 1985). We hope to cover HH2 in more detail in a future paper.

5 Energy and momentum

Neglecting projection effects and assuming a CO/H_2 abundance of 10^{-4}, the data of Snell & Edwards (1981) and Liseau & Sandell (1986) yield a blue lobe energy and momentum for the molecular flow of 2×10^{44} ergs and $1\,M_\odot$ km s^{-1} respectively. For a molecular cloud with $n_H\sim10^4$ cm^{-3}, the momentum is consistent with all the gas in a cone 0.1 pc long and 0.1 pc in base diameter (with apex at SVS13) having been accelerated to 10 km s^{-1}.

If the gas in the SVS13 jet is moving at 200 km s^{-1}, then the typical bow-shock velocity averaged over the entire HH7–11 helix is roughly 150 km s^{-1}. For such a shock the models of Raga & Bohm (1985) indicate that the gas directly affected by the dense filament is accelerated to 100 km s^{-1}, on average. If momentum is conserved in the interaction, then this shocked gas will contain the total momentum which has been deposited in the cloud and which will be transferred to a larger mass of slower moving gas further downstream in the bow-shock. Most of the energy of the shock ($\sim10^{45}$ erg for a total momentum of $1\,M_\odot$ km s^{-1}) will be radiated. If energy rather than momentum is conserved at the interaction then the situation becomes more complex, less energy is radiated and more is transferred to the molecular flow (see Beckwith, Natta & Salpeter 1983; Dyson 1984).

A lower limit of 2×10^{10} s for the age of the flow is given by the assumed jet velocity and the length of HH7–11. However, since HH7 probably does not mark the end of the blueshifted flow it is possible that this is a serious underestimate. If the true extent of the flow is taken to be the length of the red H_2 lobe or the distance to HH12, then the flow age increases to $\sim8\times10^{10}$ s (2500 yr).

Using these figures and assuming that the flow/cloud interaction has continued at a constant strength throughout the lifetime of the flow implies an average shock luminosity of $3\,L_\odot$. Considering the crudeness of the calculations, this compares well with the luminosity of HH7–11 shocks running the whole length of the helix ($\sim5\,L_\odot$) and with the estimated shock luminosity of the HH7–11 helical filament advancing at 200 km s^{-1} through a medium with $n_H\sim10^4$ cm^{-3} ($\sim10\,L_\odot$). It does seem plausible, therefore, that a precessing jet could transfer the required energy and momentum to the molecular cloud if enough of the cloud has been 'hit' by the jet filament. It is an important, if obvious point that any wavering of the jet direction has a strong effect on the efficiency of the momentum transfer between it and the molecular cloud.

Acknowledgments

We thank I. Gatley, P. W. J. L. Brand, R. P. Garden and the UKIRT staff for their assistance in making the observations. We are also grateful to R. Mundt for his criticism of an earlier

interpretation of the data, and to G. H. Herbig for providing us with photographs of the objects concerned.

References

Bally, J. & Lada, C. J., 1983. *Astrophys. J.,* **265,** 824.
Beckwith, S., Natta, A. & Salpeter, E. E., 1983. *Astrophys. J.,* **267,** 596.
Bieging, J. H. & Cohen, M., 1985. *Astrophys. J.,* **289,** L5.
Black, J. H. & Dalgarno, A., 1976. *Astrophys. J.,* **203,** 132.
Bohm, K.-H. & Solf, J., 1985. *Astrophys. J.,* **294,** 533.
Bohm, K.-H., Brugel, E. W. & Olmsted, E., 1983. *Astr. Astrophys.,* **125,** 23.
Choe, S.-U., Bohm, K.-H. & Solf, J., 1985. *Astrophys. J.,* **288,** 338.
Cohen, M. & Schwartz, R. D., 1980. *Mon. Not. R. astr. Soc.,* **191,** 165.
Cohen, M., Bieging, J. H. & Schwartz, P. R., 1982. *Astrophys. J.,* **253,** 707.
Dopita, M., Binette, L. & Schwartz, R. D., 1982. *Astrophys. J.,* **261,** 183.
Draine, B. T., Roberge, W. G. & Dalgarno, A., 1983. *Astrophys. J.,* **264,** 485.
Dyson, J. E., 1984. *Astrophys. Space Sci.,* **106,** 181.
Edwards, S. & Snell, R. L., 1983. *Astrophys. J.,* **270,** 605.
Elias, J. H., Frogel, J. A., Matthews, K. & Neugebauer, G., 1982. *Astr. J.,* **87,** 1029.
Falle, S. A. E. G. & Wilson, M. J., 1985. *Mon. Not. R. astr. Soc.,* **216,** 79.
Ferrari, A., Trussoni, E. & Zaninetti, L., 1983. *Astr. Astrophys.,* **125,** 179.
Hartmann, L. & Raymond, J. C., 1984. *Astrophys. J.,* **276,** 560.
Haschick, A. D., Moran, J. M., Rodriguez, L. F. & Ho,. P. T. P., 1983. *Astrophys. J.,* **265,** 281.
Haschick, A. D., Moran, J. M., Rodriguez, L. F., Greenfield, P. & Garcia-Barreto, J. A., 1980. *Astrophys. J.,* **237,** 26.
Herbig, G. H. & Jones, B. F., 1983. *Astr. J.,* **88,** 1040.
Jennings, R. E., Cameron, D. H. M., Cudlip, W. & Hirst, C. J., 1986. Preprint.
Jones, B. F., 1983. *Rev. Mex. Astr. Astrofis.,* **7,** 71.
Jordan, C., Brueckner, G. E., Bartoe, J.-D., Sandlin, G. D. & van Hoosier, M. E., 1978. *Astrophys. J.,* **226,** 687.
Liseau, R. & Sandell, G., 1986. *Astrophys. J.,* **304,** 459.
Morgan, J. S., Wolff, S. C., Strom, S. E. & Strom, K. M., 1984. *Astrophys. J.,* **285,** L71.
Mundt, R., 1986. In: *Protostars and Planets II,* eds Black, D. & Mattews, M., in press.
Norman, C. & Silk, J., 1979. *Astrophys. J.,* **228,** 197.
Pravdo, S. H., Rodriguez, L. F., Curiel, S., Canto, J., Torrelles, J. M., Becker, R. H. & Sellgren, K., 1985. *Astrophys. J.,* **293,** L35.
Raga, A. C. & Bohm, K.-H., 1985. *Astrophys. J. Suppl.,* **58,** 201.
Sanders, R. H., 1983. *Astrophys. J.,* **266,** 73.
Schwartz, R. D., 1978. *Astrophys. J.,* **223,** 884.
Schwartz, P. R., Bologna, J. M. & Waak, J. A., 1978. *Astrophys. J.,* **226,** 469.
Schwartz, P. R., Waak, J. A. & Smith, H. A., 1983. *Astrophys. J.,* **469,** L109.
Shull, J. M., 1978. *Astrophys. J.,* **224,** 841.
Snell, R. L. & Edwards, S., 1981. *Astrophys. J.,* **251,** 103.
Strom, S. E., Grasdalen, G. L. & Strom, K. M., 1974. *Astrophys. J.,* **191,** 111.
Strom, K. M., Strom, S. E. & Stocke, J., 1983. *Astrophys. J.,* **271,** L23.
Strom, S. E., Vrba, F. J. & Strom, K. M., 1976. *Astr. J.,* **81,** 320.
Strom, S. E., Strom, K. M., Grasdalen, G. L., Sellgren, K., Wolff, S., Morgan, J., Stocke, J. & Mundt, R., 1985. Preprint.